Phase transitions in sequential weak measurements

Wen-Long Ma,[1,3,*] Ping Wang,[1,2,3] Weng-Hang Leong,[1,3] and Ren-Bao Liu[1,3,†]

[1]*Department of Physics, The Chinese University of Hong Kong, Shatin, New Territories, Hong Kong, China*
[2]*Beijing Computational Science Research Center, Beijing 100084, China*
[3]*Centre for Quantum Coherence, The Chinese University of Hong Kong, Shatin, New Territories, Hong Kong, China*

Quantum measurement can be strong or weak, the former being important in readout and initialization of quantum objects and the latter being useful for monitoring and maneuvering quantum evolution. However, the boundary between weak and strong measurement is unclear. Here we show that a phase transition occurs in sequential quantum measurement, which unambiguously separates the weak and strong measurement by a critical value of measurement strength or duration. We formulate the probability distribution of the output of a sequence of quantum measurements as the Boltzmann distribution of an interacting spin model. The measurement results present phase transitions similar to those in the spin model. In particular the sequential commuting positive operator-valued measurement is mapped to a long-range Ising model, and a projective measurement emerges from sequential weak measurements when the strength or the number of measurements becomes above certain critical values, corresponding to the ferromagnetic phase transition of the spin model. This finding sheds insights on sequential quantum measurement, and also provides the theoretical foundation for constructing projective measurements from sequential weak measurements, which have applications in steering the quantum evolution and initializing quantum systems where strong measurement in a single shot is often not possible.

I. INTRODUCTION

Quantum measurement is fundamental to quantum mechanics [1–5]. It is also important in quantum technologies including quantum computing [6], quantum communication [7], and quantum sensing [8]. The projective measurements are the most commonly considered [6]. Generally the measurement can be the positive operator-valued measurements (POVMs) [6], including both projective measurements and weak measurements with variable measurement strength. The strong, projective measurement is useful for readout and initialization of quantum objects [9–13]; the weak measurement has been exploited for monitoring [14–21] and maneuvering quantum evolution [22,23]. In many realistic cases, such as in measuring weakly coupled nuclear spin qubits, the measurement has to be weak and sequential or continuous measurements are needed to determine the qubit state definitely [24,25]. Continuous quantum measurements have been studied by random walks in state space [26], quantum Bayesian approach [27], and stochastic path-integral formalism [28,29]. It was theoretically discovered that the qubit dynamics may be fundamentally altered by sequential weak measurement, with a phase transition between coherent oscillation and quantum Zeno effect [30]. The boundary between weak and strong measurement, however, is vague.

In this paper, we discover a phase transition between weak and strong measurement, separated by a critical measurement strength for a given time of continuous measurement or a critical measurement time for a given measurement strength. This phase transition is made explicit by the analog between the probabilities of sequential measurement outputs and thermodynamic distributions of interacting spin models [31–38]. We find that for m sequential measurements on a two-level system (TLS) [4,39–42] the sequential binary results have a probability distribution equivalent to the Boltzmann distribution of a classical spin model, with each measurement result representing a spin 1/2. Here the number of measurements m can also be understood as the measurement time of a continuous measurement. The phase transition from weak to strong measurement in this paper is different from the transition between the coherent oscillation and quantum Zeno effect [30]. The spontaneous symmetry breaking in the statistics of sequential weak measurements is also different from that in real physical devices introduced in Refs. [43,44] as an interpretation of projective quantum measurement.

II. STATISTICS OF SEQUENTIAL QUANTUM MEASUREMENTS

For m successive POVMs on a TLS (e.g., a spin-1/2 qubit), the probability to obtain the result $(\alpha_1, \alpha_2, \ldots, \alpha_m)$ is

$$
\begin{aligned}
&P(\alpha_1, \alpha_2, \ldots, \alpha_m) \\
&= \text{Tr}\big[M_{\alpha_m} \cdots M_{\alpha_2} M_{\alpha_1} |\psi_0\rangle \langle\psi_0| M_{\alpha_1}^\dagger M_{\alpha_2}^\dagger \cdots M_{\alpha_m}^\dagger \big],
\end{aligned} \quad (1)
$$

where $|\psi_0\rangle$ is the initial state of the TLS and $\{M_{\alpha_k}\}$ $(\alpha_k = \pm 1)$ is the set of POVM operators for the kth measurement satisfying $\sum_{\alpha_k} M_{\alpha_k}^\dagger M_{\alpha_k} = I$. Here the evolution of the TLS between measurements has been absorbed into the POVM operators.

*Present address: Department of Applied Physics, Yale University, New Haven, Connecticut 06511, USA.
†Corresponding author: rbliu@cuhk.edu.hk

Below we will show how to map measurement statistics to the Boltzmann distribution of a classical lattice spin model, i.e.,

$$P(\alpha_1, \alpha_2, \ldots, \alpha_m) = \exp\left[-H(\alpha_1, \alpha_2, \ldots, \alpha_m)\right], \quad (2)$$

where $H(\alpha_1, \alpha_2, \ldots, \alpha_m)$ is the Hamiltonian of the lattice spin model with α_k denoting the kth lattice spin (temperature absorbed into the Hamiltonian). Obviously, the Hamiltonian is $H(\alpha_1, \alpha_2, \ldots, \alpha_m) = -\ln[P(\alpha_1, \alpha_2, \ldots, \alpha_m)]$. Below we focus on two exactly solvable cases.

A. Case I: Sequential projective measurements

For m successive projective measurements on the TLS,

$$M_{\alpha_k} = \tfrac{1}{2}[I + \alpha_k(\hat{\boldsymbol{\sigma}} \cdot \boldsymbol{n}_k)] = |\alpha_k\rangle\langle\alpha_k|, \quad (3)$$

where $\hat{\boldsymbol{\sigma}} = (\sigma_x, \sigma_y, \sigma_z)$ are the Pauli matrices of the TLS, $\boldsymbol{n}_k$ is the unit vector of the kth measurement axis, and $|\alpha_k\rangle$ is the eigenstate of $\hat{\boldsymbol{\sigma}} \cdot \boldsymbol{n}_k$ with eigenvalue α_k. Suppose the initial state of the TLS is $|\psi_0\rangle = |\alpha_0\rangle$ with $\alpha_0 = \pm 1$. The probability distribution of the measurement results is [4] (see Appendix A 1)

$$P_{\mathrm{I}} = \frac{1}{2^m} \prod_{k=1}^{m} [1 + \cos(\phi_{k-1,k})\alpha_{k-1}\alpha_k], \quad (4)$$

where $\phi_{k-1,k} = \arccos(\boldsymbol{n}_{k-1} \cdot \boldsymbol{n}_k) \in [0, \pi]$ denotes the angle between the $(k-1)$th and kth measurement axes.

The probability distribution for sequential projective measurements [Eq. (4)] is exactly the normalized partition function of a classical one-dimensional (1D) Ising model with nearest-neighbor interaction (see Appendix A 2):

$$H_{\mathrm{I}} = -\sum_{k=1}^{m} J_{k-1,k}\alpha_{k-1}\alpha_k, \quad (5)$$

where $J_{k-1,k} = \tanh^{-1}[\cos(\phi_{k-1,k})]$. If $\phi_{k-1,k} \in [0, \pi/2)$, $J_{k-1,k} > 0$ corresponding to a ferromagnetic coupling; if $\phi_{k-1,k} \in (\pi/2, \pi]$, $J_{k-1,k} < 0$ corresponding to an antiferromagnetic coupling; if $\phi_{k-1,k} = \pi/2$, $J_{k-1,k} = 0$ corresponding to the noninteracting case.

The correlation function between the results of the jth measurement and the $(j+n)$th measurement is the same as the correlation function of the 1D Ising model [Eq. (5)]:

$$\langle \alpha_j \alpha_{j+n} \rangle = \prod_{k=j+1}^{j+n} \tanh(J_{k-1,k}) = \prod_{k=j+1}^{j+n} \cos(\phi_{k-1,k}). \quad (6)$$

Consider the specific case where $J_{0,1} = J_{1,2} \cdots = J_{m-1,m} = J$ and $\phi_{0,1} = \phi_{1,2} \cdots = \phi_{m-1,m} = \phi$. For the ferromagnetic coupling ($J > 0$, i.e., $0 < \cos\phi < 1$), the correlation function $\langle \alpha_j \alpha_{j+n} \rangle = \cos^n(\phi)$ shows an exponential decay with respect to the distance between the two lattice spins, indicating a paramagnetic phase. If $\cos\phi = 1$, the correlation function is a constant ($\langle \alpha_j \alpha_{j+n} \rangle = 1$), indicating a ferromagnetic phase transition for infinite coupling ($J = +\infty$) or zero temperature. This phase transition can be intuitively understood: The condition $\cos\phi = 1$ indicates that all the projective measurements are along the same axis, therefore the first measurement collapses the TLS into an eigenstate of the projective operator and all the subsequent measurements

will give the same result. The case for the antiferromagnetic coupling is similar, except that at the antiferromagnetic phase transition point ($\cos\phi = -1$ and $J = -\infty$) the correlation function becomes $\langle \alpha_j \alpha_{j+n} \rangle = (-1)^n$.

B. Case II: Sequential commuting POVMs

Consider m sequential commuting POVMs [26] with

$$M_{\alpha_k} = \frac{1}{\sqrt{2}}[\cos(\theta_k)I + \sin(\theta_k)\alpha_k\sigma_z], \quad (7)$$

where $\theta_k \in [0, \pi/4]$. The measurement strength is defined by $\lambda_k = \sin^2(2\theta_k)$. When λ_k increases from zero to one, the kth measurement continuously changes from weak measurement to strong projective measurement.

Suppose the initial state of the TLS is $|\psi_0\rangle = C_0^+|+1\rangle + C_0^-|-1\rangle$ with $|\pm 1\rangle$ being the eigenstates of σ_z and $|C_0^+|^2 + |C_0^-|^2 = 1$. The un-normalized state of the TLS after m measurements is

$$|\psi_m\rangle = M_{\alpha_m} \cdots M_{\alpha_2} M_{\alpha_1}|\psi_0\rangle = C_m^+|+1\rangle + C_m^-|-1\rangle, \quad (8)$$

with

$$\begin{aligned} C_m^{\pm} &= \frac{1}{\sqrt{2}}[\cos(\theta_m) \pm \sin(\theta_m)\alpha_m]C_{m-1}^{\pm} \\ &= \frac{C_0^{\pm}}{2^{m/2}} \prod_{k=1}^{m} [\cos(\theta_k) \pm \sin(\theta_k)\alpha_k], \end{aligned} \quad (9)$$

and the normalized state is $|\psi'_m\rangle = |\psi_m\rangle/\sqrt{\langle\psi_m|\psi_m\rangle}$. Denote the Bloch vector components of the final state as $r_m^i = \langle\sigma_i\rangle = \langle\psi'_m|\sigma_i|\psi'_m\rangle$ $(i = x, y, z)$ $(r_m = 1$ for a pure state). The probability distribution for the measurement results is (see Appendix B 1)

$$\begin{aligned} P_{\mathrm{II}} = \langle\psi_m|\psi_m\rangle = \frac{1}{2^{m+1}}\Bigg[&\left(1 + r_0^z\right)\prod_{k=1}^{m}(1 + \sqrt{\lambda_k}\alpha_k) \\ &+ \left(1 - r_0^z\right)\prod_{k=1}^{m}(1 - \sqrt{\lambda_k}\alpha_k)\Bigg], \end{aligned} \quad (10)$$

where $r_0^z = |C_0^+|^2 - |C_0^-|^2$.

The lattice spin Hamiltonian corresponding to the probability distribution of sequential POVMs is

$$\begin{aligned} H_{\mathrm{II}} = -\ln\Bigg\{ \frac{1}{2^{m+1}}\Bigg[&\left(1 + r_0^z\right)\prod_{k=1}^{m}(1 + \sqrt{\lambda}\alpha_k) \\ &+ \left(1 - r_0^z\right)\prod_{k=1}^{m}(1 - \sqrt{\lambda}\alpha_k)\Bigg]\Bigg\}. \end{aligned} \quad (11)$$

Here we have assumed that $\lambda_1 = \lambda_2 = \cdots = \lambda_m = \lambda$. We identify the order parameter as the measurement polarization $X = q/m - 1/2$ with q being the number of measurements with result $\alpha = +1$. Then the probability distribution of X is

$$\begin{aligned} P(X) = [(1-\lambda)/4]^{m/2}C_m^{m(X+1/2)} \\ \times \left\{\cosh[\ln(\eta)mX] + r_0^z \sinh[\ln(\eta)mX]\right\}, \end{aligned} \quad (12)$$
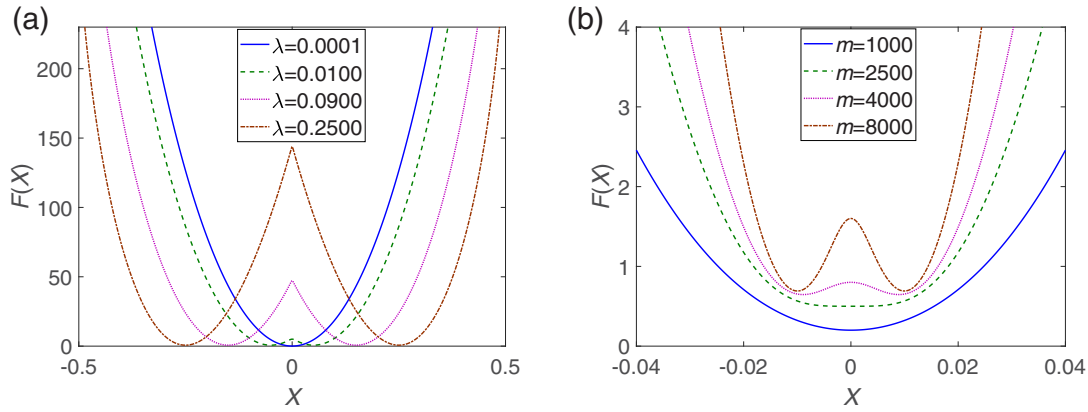
FIG. 1. Free energy of the spin model corresponding to a sequential POVM. (a) Free energy as a function of measurement polarization X for different measurement strengths λ with the measurement time $m = 1000$. (b) Free energy as a function of X for different m with $\lambda = 0.0004$. Here we use the initial state of the TLS with $r_0^z = 0$.

where C_m^j is the binomial coefficient and $\eta = (1+\sqrt{\lambda})/(1-\sqrt{\lambda})$. Define the free energy as

$$F(X) = -\ln[P(X)] \approx m\varphi(X)$$
$$- \ln\left\{\cosh[\ln(\eta)mX] + r_0^z \sinh[\ln(\eta)mX]\right\}, \quad (13)$$

where $\varphi(X) = (1/2+X)\ln(1/2+X) + (1/2-X)\ln(1/2-X)$ [45]. In $F(X)$, the first and the second parts represent the entropy and the internal energy, respectively. $F(X)$ takes the minimum when $\partial F(X_{min})/\partial X = 0$. After solving for X_{min}, the z component of the Bloch vector of the TLS after m
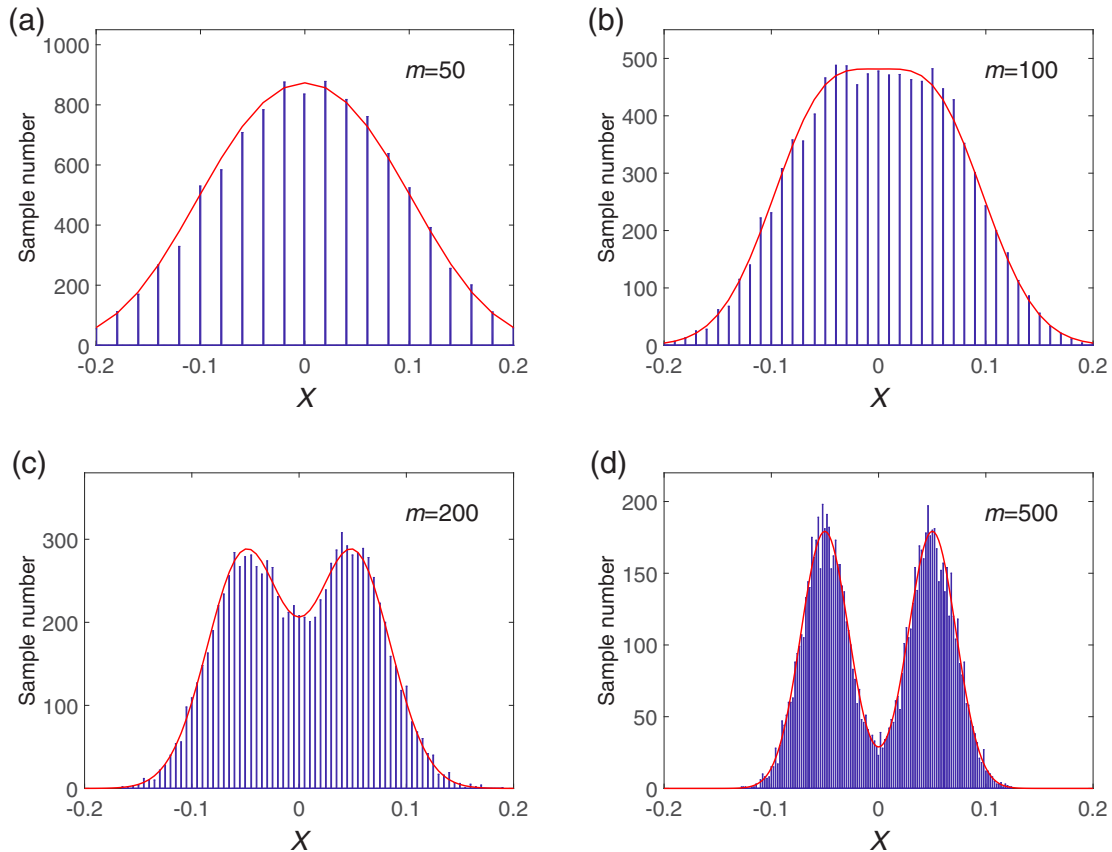

FIG. 2. The histogram of the number of samples with respect to the measurement polarization X in the Monte Carlo simulation of sequential POVMs in case II for different measurement times: (a) $m = 50$, (b) $m = 100$, (c) $m = 200$, and (d) $m = 500$. The red solid lines represent the exact probability distribution in Eq. (10). The measurement strength is $\lambda = 0.01$. The simulation contains 10^4 samples of sequential POVMs from the same initial state ($r_0^z = 0$).
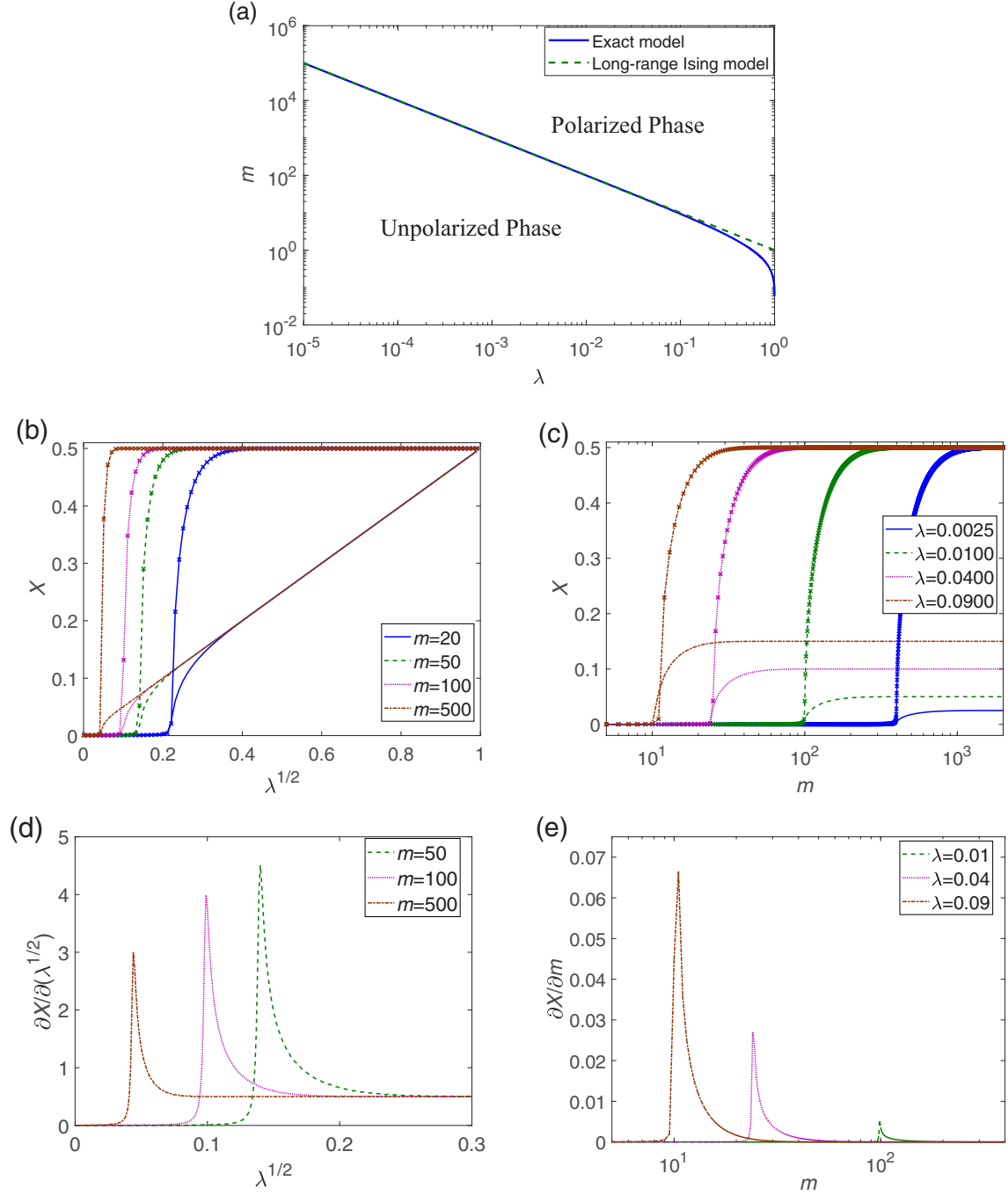
FIG. 3. Phase transitions of sequential weak measurement. (a) Critical measurement time m_C as a function of the measurement strength λ. (b), (d) The measurement polarization X and $\partial X/\partial\sqrt{\lambda}$ as functions of $\sqrt{\lambda}$ for different measurement times m. (c), (e) X and $\partial X/\partial\sqrt{\lambda}$ as functions of m for different λ. In (b)–(d), the lines without (with) crosses represent the results from the exact model (the long-range Ising model). Here we use the initial state with $r_0^z = 0$.

POVMs is

$$r_m^z = \frac{\sinh\left[\ln\left(\eta\right)mX_{\min}\right] + r_0^z\cosh\left[\ln\left(\eta\right)mX_{\min}\right]}{\cosh\left[\ln\left(\eta\right)mX_{\min}\right] + r_0^z\sinh\left[\ln\left(\eta\right)mX_{\min}\right]}, \quad (14)$$

and the x and y components are $r_m^{x/y} = r_0^{x/y}/$ $\{\cosh[\ln(\eta)mX_{\min}] + r_0^z\sinh[\ln(\eta)mX_{\min}]\}$.

To simplify the discussion, we assume that the initial states of the TLS lie in the equatorial plane of the Bloch sphere with

$r_0^z = 0$, then the spin Hamiltonian is

$$H_{\mathrm{II}} = -\ln\left\{\frac{1}{2}\left[\prod_{k=1}^{m}(1+\sqrt{\lambda}\alpha_k) + \prod_{k=1}^{m}(1-\sqrt{\lambda}\alpha_k)\right]\right\}, \quad (15)$$

where we have dropped the constant $\propto m$ in H_{II}. For weak measurement ($\lambda \ll 1$), the above Hamiltonian is equivalent to the long-range ferromagnetic Ising model (see Appendix B 6)

up to leading-order terms ($\propto \lambda$):

$$H_{\text{II}} \approx -\lambda \sum_{j<k}^{m} \alpha_j \alpha_k. \tag{16}$$

The free energy $F(X)$ [Eq. (13)] depends on both the measurement strength λ and the measurement time m. For a fixed m, $F(X)$ shows spontaneous symmetry breaking as λ is increased [Fig. 1(a)]. Similarly, for a fixed m, $F(X)$ also shows spontaneous symmetry breaking as m is increased [Fig. 1(b)]. This implies a phase transition between the unpolarized phase and the polarized phase in the two-dimensional parameter space (λ, m), which is verified by a Monte Carlo simulation of 10^4 samples of sequential POVMs (Fig. 2).

The distance between the two valleys in the polarized phase increases with the measurement strength λ but is independent of the measurement time m. If $m\ln^2(\eta) < 4$, $F(X)$ has only one minimum at $X = 0$ corresponding to the unpolarized phase, while, if $m\ln^2(\eta) > 4$, $F(X)$ has two minima located within $(-1/2, 0)$ and $(1/2, 0)$ corresponding to the polarized phase. So the phase transition occurs when m and λ satisfy (see Appendix B 2)

$$m\ln^2(\eta) = m\ln^2\left(\frac{1+\sqrt{\lambda}}{1-\sqrt{\lambda}}\right) = 4. \tag{17}$$

For a fixed λ, the critical measurement time is $m_c = 4/\ln^2[(1+\sqrt{\lambda})/(1-\sqrt{\lambda})]$; likewise, for a fixed m, the critical measurement strength is $\lambda_c = \tanh^2(m^{-1/2})$. For weak measurement ($\lambda \ll 1$), the phase boundary is $m\lambda = 1$, which coincides with that for the long-range Ising model [Eq. (16)] [38] and implies that the weaker the measurement strength the larger the measurement time that is needed to observe the phase transition [Fig. 3(a)].

However, the order parameter X as a function of the measurement time m and measurement strength λ is quite different for the exact spin model than for the long-range Ising model [Figs. 3(b) and 3(c)]. In the exact model, for a fixed m, X quickly increases above the critical measurement strength λ_c and then increases linearly with $\sqrt{\lambda}$ as $X = \pm\sqrt{\lambda}/2$; for a fixed λ, X also quickly increases above the critical measurement time m_c and approaches the constant $X = \pm\sqrt{\lambda}/2$ as m is further increased. This implies that in the polarized phase X is proportional to $\sqrt{\lambda}$ but independent of m. Moreover, $\partial X/\partial\sqrt{\lambda}$ or $\partial X/\partial m$ shows a finite jump at the critical points [Figs. 3(d) and 3(e)], which is a signature of second-order phase transitions. However, for the long-range ferromagnetic Ising model, it is $m\lambda$ that influences the ferromagnetic phase transition, and $X = \pm1/2$ in the ferromagnetic phase.

Moreover, the final state polarization r_m^z of the TLS also shows a phase-transition behavior depending on m and λ

[24,25] (see Appendix B 3). For a fixed m, r_m^z keeps almost unchanged compared to the initial one with λ below the critical value λ_c but quickly becomes fully polarized to the north or south pole as λ increases above λ_c. Similar behavior is observed for a fixed λ and increasing m. When the state polarization begins, the TLS has the same probability to be polarized to the north or south pole, and it has to decide which path to choose. This is quite similar to the spontaneous symmetry breaking in statistical physics.

If the initial state of the TLS $|\psi_0\rangle$ is in the north or south pole with $r_0^z = \pm1$, the probability distribution is mapped to m independent paramagnetic classical spins, and there is no phase transition in this case. If $|\psi_0\rangle$ is on the Bloch sphere with $|r_0^z| \in (0, 1)$, for weak measurement ($\lambda \ll 1$), the probability distribution can be mapped to the long-range ferromagnetic Ising model under an external magnetic field. The measurement polarization X as a function of m and λ changes more and more smoothly as $|r_0^z|$ increases and the phase-transition behaviors gradually disappear.

Moreover, we numerically demonstrate that the phase transition behaviors still persist even if there are small fluctuations of the measurement strength λ_k for sequential POVMs and if sequential POVM operators $\{M_{\alpha_k}\}$ do not exactly commute [46].

III. CONCLUSIONS AND OUTLOOKS

We establish the connections between the probability distribution of sequential quantum measurement on a TLS and the statistical mechanics of classical spin models. Therefore, the statistics and phase transitions of the spin chains can be effectively simulated by measuring a single qubit. For sequential projective measurements, the measurement results simulate the 1D Ising model with nearest-neighbor interactions; for sequential commuting POVMs, the measurement is mapped to ferromagnetic long-range Ising models. We find a polarized-to-unpolarized phase transition in sequential POVMs dependent on the measurement time and measurement strength.

In this paper, we focus on the mapping of the measurement statistics of binary-outcome POVMs on a TLS to the statistics of classical Ising models with spin $1/2$. An interesting problem is to study the measurement statistics of general multioutcome POVMs on a TLS or a multilevel system (see Appendix D), which may be mapped to the statistics of classical Ising models of higher spins that exhibit richer phase transition behaviors [47,48].

ACKNOWLEDGMENT

APPENDIX A: SEQUENTIAL PROJECTIVE MEASUREMENTS

1. Derivation of the probability distribution

In case I, the projective measurements on the TLS are defined as

$$M_{\alpha_k} = \tfrac{1}{2}[I + \alpha_k(\hat{\boldsymbol{\sigma}} \cdot \boldsymbol{n}_k)] = |\alpha_k\rangle\langle\alpha_k|, \tag{A1}$$

where $\alpha_k = \pm 1$ represents the binary measurement results. The probability to obtain the measurement result $(\alpha_1, \alpha_2, \ldots, \alpha_m)$ is

$$P(\alpha_1, \alpha_2, \ldots, \alpha_m) = \mathrm{Tr}\big[\mathcal{M}_{\alpha_m} \cdots \mathcal{M}_{\alpha_2} \mathcal{M}_{\alpha_1} \rho_0\big], \tag{A2}$$

where $\rho_0 = (I + \alpha_0 \hat{\boldsymbol{\sigma}} \cdot \boldsymbol{n}_0)/2$ and $\mathcal{M}_{\alpha_k}(\bullet) = M_{\alpha_k}(\bullet) M_{\alpha_k}^{\dagger}$. For the Pauli matrices, we have the following relation:

$$(I + \alpha_1 \hat{\boldsymbol{\sigma}} \cdot \boldsymbol{n}_1)(I + \alpha_0 \hat{\boldsymbol{\sigma}} \cdot \boldsymbol{n}_0)(I + \alpha_1 \hat{\boldsymbol{\sigma}} \cdot \boldsymbol{n}_1) = 2(I + \alpha_0 \alpha_1 \boldsymbol{n}_1 \cdot \boldsymbol{n}_0)(I + \alpha_1 \hat{\boldsymbol{\sigma}} \cdot \boldsymbol{n}_1), \tag{A3}$$

where we have used

$$
\begin{aligned}
(\hat{\boldsymbol{\sigma}} \cdot \boldsymbol{n}_1)(\hat{\boldsymbol{\sigma}} \cdot \boldsymbol{n}_0) &= \boldsymbol{n}_1 \cdot \boldsymbol{n}_0 + i\hat{\boldsymbol{\sigma}} \cdot (\boldsymbol{n}_1 \times \boldsymbol{n}_0), \\
(\hat{\boldsymbol{\sigma}} \cdot \boldsymbol{n}_1)(\hat{\boldsymbol{\sigma}} \cdot \boldsymbol{n}_0)(\hat{\boldsymbol{\sigma}} \cdot \boldsymbol{n}_1) &= 2(\boldsymbol{n}_1 \cdot \boldsymbol{n}_0)(\hat{\boldsymbol{\sigma}} \cdot \boldsymbol{n}_1) - \hat{\boldsymbol{\sigma}} \cdot \boldsymbol{n}_0,
\end{aligned}
\tag{A4}
$$

so the probability distribution can be directly derived as

$$
\begin{aligned}
P(\alpha_1, &\alpha_2, \ldots, \alpha_m) \\
&= \frac{1}{2^{2m+1}} \mathrm{Tr}[(I + \alpha_m \hat{\boldsymbol{\sigma}} \cdot \boldsymbol{n}_m) \cdots (I + \alpha_1 \hat{\boldsymbol{\sigma}} \cdot \boldsymbol{n}_1)(I + \alpha_0 \hat{\boldsymbol{\sigma}} \cdot \boldsymbol{n}_0)(I + \alpha_1 \hat{\boldsymbol{\sigma}} \cdot \boldsymbol{n}_1) \cdots (I + \alpha_m \hat{\boldsymbol{\sigma}} \cdot \boldsymbol{n}_m)] \\
&= \frac{1}{2^{2m}} (I + \alpha_0 \alpha_1 \boldsymbol{n}_1 \cdot \boldsymbol{n}_0) \mathrm{Tr}[(I + \alpha_m \hat{\boldsymbol{\sigma}} \cdot \boldsymbol{n}_m) \cdots (I + \alpha_2 \hat{\boldsymbol{\sigma}} \cdot \boldsymbol{n}_2)(I + \alpha_1 \hat{\boldsymbol{\sigma}} \cdot \boldsymbol{n}_1)(I + \alpha_2 \hat{\boldsymbol{\sigma}} \cdot \boldsymbol{n}_2) \cdots (I + \alpha_m \hat{\boldsymbol{\sigma}} \cdot \boldsymbol{n}_m)] \\
&= \frac{1}{2^m} \prod_{k=1}^{m} [1 + \cos(\phi_{k-1,k}) \alpha_{k-1} \alpha_k],
\end{aligned}
\tag{A5}
$$

where $\phi_{k-1,k} = \arccos(\boldsymbol{n}_{k-1} \cdot \boldsymbol{n}_k) \in [0, \pi]$.

2. 1D Ising model with nearest-neighbor interactions

The Hamiltonian of the 1D Ising model with nearest-neighbor interactions is

$$H_{\mathrm{I}}(\alpha_1, \alpha_2, \ldots, \alpha_m) = -\sum_{k=1}^{m} J_{k-1,k} \alpha_{k-1} \alpha_k. \tag{A6}$$

To be consistent with the quantum measurement model, we take the open boundary condition with $\alpha_0 = \pm 1$. In thermal equilibrium, the probability for the m spins to be in the configuration $(\alpha_1, \alpha_2, \ldots, \alpha_m)$ obeys the Boltzmann distribution

$$
\begin{aligned}
P'(\alpha_1, \alpha_2, \ldots, \alpha_m) &= \exp\left(\sum_{k=1}^{m} J_{k-1,k} \alpha_{k-1} \alpha_k\right) \\
&= \left[\cosh(\alpha_0 J_{0,1}) \prod_{k=2}^{m} \cosh(J_{k-1,k})\right] \prod_{k=1}^{m} [1 + \tanh(J_{k-1,k}) \alpha_{k-1} \alpha_k],
\end{aligned}
\tag{A7}
$$

where we have set $\beta = 1/T = 1$. The partition function of the 1D Ising model is

$$Z = \sum_{\{\alpha_1, \alpha_2, \ldots, \alpha_m\}} P'(\alpha_1, \alpha_2, \ldots, \alpha_m) = \sum_{\alpha_1 = \pm 1} \sum_{\alpha_2 = \pm 1} \cdots \sum_{\alpha_m = \pm 1} e^{J_{01} \alpha_0 \alpha_1} e^{J_{12} \alpha_1 \alpha_2} \cdots e^{J_{m-1,m} \alpha_{m-1} \alpha_m}, \tag{A8}$$

where $e^{J_{k-1,k} \alpha_{k-1} \alpha_k}$ can be written as a matrix as follows:

$$e^{J_{k-1,k} \alpha_{k-1} \alpha_k} = \begin{bmatrix} e^{J_{k-1,k}} & e^{-J_{k-1,k}} \\ e^{-J_{k-1,k}} & e^{J_{k-1,k}} \end{bmatrix} = \begin{bmatrix} 1 & 1 \\ 1 & -1 \end{bmatrix} \begin{bmatrix} \cosh(J_{k-1,k}) & 0 \\ 0 & \sinh(J_{k-1,k}) \end{bmatrix} \begin{bmatrix} 1 & 1 \\ 1 & -1 \end{bmatrix}, \tag{A9}$$

so we have

$$
\begin{aligned}
e^{J_{01} \alpha_0 \alpha_1} &e^{J_{12} \alpha_1 \alpha_2} \cdots e^{J_{m-1,m} \alpha_{m-1} \alpha_m} \\
&= \begin{bmatrix} e^{J_{01} \alpha_0} & 0 \\ 0 & e^{-J_{01} \alpha_0} \end{bmatrix} \begin{bmatrix} e^{J_{12}} & e^{-J_{12}} \\ e^{-J_{12}} & e^{J_{12}} \end{bmatrix} \cdots \begin{bmatrix} e^{J_{m-1,m}} & e^{-J_{m-1,m}} \\ e^{-J_{m-1,m}} & e^{J_{m-1,m}} \end{bmatrix} \\
&= 2^{m-2} \begin{bmatrix} e^{J_{01} \alpha_0} & 0 \\ 0 & e^{-J_{01} \alpha_0} \end{bmatrix} \begin{bmatrix} 1 & 1 \\ 1 & -1 \end{bmatrix} \left\{ \prod_{k=2}^{m} \begin{bmatrix} \cosh(J_{k-1,k}) & 0 \\ 0 & \sinh(J_{k-1,k}) \end{bmatrix} \right\} \begin{bmatrix} 1 & 1 \\ 1 & -1 \end{bmatrix} \\
&= 2^{m-2} \begin{bmatrix} e^{J_{01} \alpha_0} \left(\prod_{k=2}^{m} \cosh(J_{k-1,k}) + \prod_{k=2}^{m} \sinh(J_{k-1,k}) \right) & e^{J_{01} \alpha_0} \left(\prod_{k=2}^{m} \cosh(J_{k-1,k}) - \prod_{k=2}^{m} \sinh(J_{k-1,k}) \right) \\ e^{-J_{01} \alpha_0} \left(\prod_{k=2}^{m} \cosh(J_{k-1,k}) - \prod_{k=2}^{m} \sinh(J_{k-1,k}) \right) & e^{-J_{01} \alpha_0} \left(\prod_{k=2}^{m} \cosh(J_{k-1,k}) + \prod_{k=2}^{m} \sinh(J_{k-1,k}) \right) \end{bmatrix}.
\end{aligned}
\tag{A10}
$$

The partition function is the summation of all the elements of the above matrix:

$$Z = \sum_{\alpha_1 = \pm 1} \sum_{\alpha_m = \pm 1} \langle \alpha_1 | e^{J_{01}\alpha_0\alpha_1} e^{J_{12}\alpha_1\alpha_2} \cdots e^{J_{m-1,m}\alpha_{m-1}\alpha_m} | \alpha_m \rangle = 2^m \cosh(\alpha_0 J_{0,1}) \prod_{k=2}^{m} \cosh(J_{k-1,k}). \tag{A11}$$

So the normalized probability distribution is

$$P(\alpha_1, \alpha_2, \ldots, \alpha_m) = \frac{P'(\alpha_1, \alpha_2, \ldots, \alpha_m)}{Z} = \prod_{k=1}^{m} [1 + \tanh(J_{k-1,k})\alpha_{k-1}\alpha_k]. \tag{A12}$$

The correlation function between the jth spin ($j \geqslant 1$) and the $(j + n)$th ($n \leqslant m - j$) spin is obtained by taking the derivatives of the partition function with respect to the coupling strength:

$$\begin{aligned}
\langle \alpha_j \alpha_{j+n} \rangle &= \langle \alpha_j \alpha_{j+1} \alpha_{j+1} \alpha_{j+2} \cdots \alpha_{j+n-1} \alpha_{j+n} \rangle \\
&= \frac{1}{Z} \sum_{\{\alpha_1, \alpha_2, \ldots, \alpha_m\}} \alpha_j \alpha_{j+1} \alpha_{j+1} \alpha_{j+2} \cdots \alpha_{j+n-1} \alpha_{j+n} \exp\left(\sum_{k=1}^{m} J_{k-1,k} \alpha_{k-1} \alpha_k \right) \\
&= \frac{\partial}{\partial J_{j,j+1}} \frac{\partial}{\partial J_{j+1,j+2}} \cdots \frac{\partial}{\partial J_{j+n-1,j+n}} \ln(Z) \\
&= \prod_{k=j+1}^{j+n} \tanh(J_{k-1,k}).
\end{aligned} \tag{A13}$$

APPENDIX B: SEQUENTIAL COMMUTING POVMs

1. Derivation of the probability distribution

In the main text, we have directly derived the probability distribution by considering the changes of the TLS states caused by sequential POVMs. Here we will give equivalent derivations using the density matrix formulism. In case II, the POVMs on the TLS are defined as

$$M_{\alpha_k} = \frac{1}{\sqrt{2}}[\cos(\theta_k)I + \sin(\theta_k)\alpha_k \sigma_z], \tag{B1}$$

where $\theta_k \in [0, \pi/4]$. The measurement strength λ_k is defined by $\lambda_k = \sin^2(2\theta_k)$.

After m successive commuting POVMs, the un-normalized density matrix of the TLS is

$$\rho_k = \mathcal{M}_{\alpha_k} \cdots \mathcal{M}_{\alpha_2} \mathcal{M}_{\alpha_1} \rho_0 = A_k + B_k \hat{\boldsymbol{\sigma}} \cdot \boldsymbol{n}_k, \tag{B2}$$

and the normalized density matrix is $\rho'_k = \rho_k/\text{Tr}(\rho_k) = (I + r_k \hat{\boldsymbol{\sigma}} \cdot \boldsymbol{n}_k)/2$ with $r_k = B_k/A_k$ and $\boldsymbol{n}_k$ denoting the length and direction of the Bloch vector, respectively. The relation between ρ_k and ρ_{k-1} is fully captured by the transfer matrix

$$\begin{bmatrix} A_k \\ B_k^x \\ B_k^y \\ B_k^z \end{bmatrix} = \frac{1}{2} \begin{bmatrix} 1 & 0 & 0 & \sqrt{\lambda_k}\alpha_k \\ 0 & \sqrt{1-\lambda_k} & 0 & 0 \\ 0 & 0 & \sqrt{1-\lambda_k} & 0 \\ \sqrt{\lambda_k}\alpha_k & 0 & 0 & 1 \end{bmatrix} \begin{bmatrix} A_{k-1} \\ B_{k-1}^x \\ B_{k-1}^y \\ B_{k-1}^z \end{bmatrix}. \tag{B3}$$

Note that the above transfer matrix can be diagonalized with the same transformation matrix for any k, so we have

$$\begin{aligned}
\begin{bmatrix} A_m \\ B_m^x \\ B_m^y \\ B_m^z \end{bmatrix} &= \frac{1}{2^{m+1}} \begin{bmatrix} 1 & 0 & 0 & 1 \\ 0 & \sqrt{2} & 0 & 0 \\ 0 & 0 & \sqrt{2} & 0 \\ 1 & 0 & 0 & -1 \end{bmatrix} \left\{ \prod_{k=1}^{m} \begin{bmatrix} 1+\sqrt{\lambda_k}\alpha_k & 0 & 0 & 0 \\ 0 & \sqrt{1-\lambda_k} & 0 & 0 \\ 0 & 0 & \sqrt{1-\lambda_k} & 0 \\ 0 & 0 & 0 & 1-\sqrt{\lambda_k}\alpha_k \end{bmatrix} \right\} \\
&\quad \times \begin{bmatrix} 1 & 0 & 0 & 1 \\ 0 & \sqrt{2} & 0 & 0 \\ 0 & 0 & \sqrt{2} & 0 \\ 1 & 0 & 0 & -1 \end{bmatrix} \begin{bmatrix} A_0 \\ B_0^x \\ B_0^y \\ B_0^z \end{bmatrix},
\end{aligned} \tag{B4}$$

with the initial condition $\rho_0 = (I + r_0 \hat{\boldsymbol{\sigma}} \cdot \boldsymbol{n}_0)/2$, i.e., $(A_0, B_0^x, B_0^y, B_0^z) = (1, r_0^x, r_0^y, r_0^z)/2$, and we have the solution

$$A_m = \frac{1}{2^{m+2}} \left[\left(1 + r_0^z\right) \prod_{k=1}^{m} (1 + \sqrt{\lambda_k} \alpha_k) + \left(1 - r_0^z\right) \prod_{k=1}^{m} (1 - \sqrt{\lambda_k} \alpha_k) \right],$$

$$B_m^x = \frac{1}{2^{m+1}} r_0^x \prod_{k=1}^{m} \sqrt{1 - \lambda_k},$$

$$B_m^y = \frac{1}{2^{m+1}} r_0^y \prod_{k=1}^{m} \sqrt{1 - \lambda_k},$$

$$B_m^z = \frac{1}{2^{m+2}} \left[\left(1 + r_0^z\right) \prod_{k=1}^{m} (1 + \sqrt{\lambda_k} \alpha_k) - \left(1 - r_0^z\right) \prod_{k=1}^{m} (1 - \sqrt{\lambda_k} \alpha_k) \right], \tag{B5}$$

so the probability to obtain the measurement result $(\alpha_1, \alpha_2, \ldots, \alpha_m)$ is

$$P_{\mathrm{II}}(\alpha_1, \alpha_2, \ldots, \alpha_m) = \mathrm{Tr}[\rho_m] = 2A_m$$

$$= \frac{1}{2^{m+1}} \left[\left(1 + r_0^z\right) \prod_{k=1}^{m} (1 + \sqrt{\lambda_k} \alpha_k) + \left(1 - r_0^z\right) \prod_{k=1}^{m} (1 - \sqrt{\lambda_k} \alpha_k) \right], \tag{B6}$$

and the density matrix of the TLS after m measurements is $\rho'_m = (I + r_m \hat{\boldsymbol{\sigma}} \cdot \boldsymbol{n}_m)/2$ with

$$r_m^x = \frac{B_m^x}{A_m} = \frac{2 r_0^x \prod_{k=1}^{m} \sqrt{1 - \lambda_k}}{\left(1 + r_0^z\right) \prod_{k=1}^{m} (1 + \sqrt{\lambda_k} \alpha_k) - \left(1 - r_0^z\right) \prod_{k=1}^{m} (1 - \sqrt{\lambda_k} \alpha_k)},$$

$$r_m^y = \frac{B_m^y}{A_m} = \frac{2 r_0^y \prod_{k=1}^{m} \sqrt{1 - \lambda_k}}{\left(1 + r_0^z\right) \prod_{k=1}^{m} (1 + \sqrt{\lambda_k} \alpha_k) + \left(1 - r_0^z\right) \prod_{k=1}^{m} (1 - \sqrt{\lambda_k} \alpha_k)}, \tag{B7}$$

$$r_m^z = \frac{B_m^z}{A_m} = \frac{\left(1 + r_0^z\right) \prod_{k=1}^{m} (1 + \sqrt{\lambda_k} \alpha_k) - \left(1 - r_0^z\right) \prod_{k=1}^{m} (1 - \sqrt{\lambda_k} \alpha_k)}{\left(1 + r_0^z\right) \prod_{k=1}^{m} (1 + \sqrt{\lambda_k} \alpha_k) + \left(1 - r_0^z\right) \prod_{k=1}^{m} (1 - \sqrt{\lambda_k} \alpha_k)}.$$

It can be easily shown that if the initial state of the TLS is a pure state with $r_0 = \pm\sqrt{(r_0^x)^2 + (r_0^y)^2 + (r_0^z)^2} = \pm 1$, then the final state of the TLS after m POVMs is always a pure state with $r_m = \pm\sqrt{(r_m^x)^2 + (r_m^y)^2 + (r_m^z)^2} = \pm 1$.

2. Minimum of free energy and phase transitions

Assume that all the sequential measurements are the same with $\lambda_1 = \lambda_2 = \cdots = \lambda_m = \lambda$. The probability distribution becomes

$$P_{\mathrm{II}}(\alpha_1, \alpha_2, \ldots, \alpha_m) = \frac{1}{2^{m+1}} \left[\left(1 + r_0^z\right) \prod_{k=1}^{m} (1 + \sqrt{\lambda} \alpha_k) + \left(1 - r_0^z\right) \prod_{k=1}^{m} (1 - \sqrt{\lambda} \alpha_k) \right]. \tag{B8}$$

The measurement polarization is defined as $X = q/m - 1/2$ with q being the number of measurements with result $\alpha = +1$. Then the probability distribution of X is

$$P(X) = [(1 - \lambda)/4]^{m/2} C_m^{m(X+1/2)} \left\{ \cosh\left[\ln(\eta) m X\right] + r_0^z \sinh\left[\ln(\eta) m X\right] \right\}, \tag{B9}$$

where $\eta = (1 + \sqrt{\lambda})/(1 - \sqrt{\lambda})$. In Fig. 4, we plot $P(X)$ as a function of X for different measurement times m, measurement strength λ, or initial state polarization of the TLS r_0^z. First we consider the unpolarized initial state with $r_0^z = 0$: for a fixed m, $P(X)$ has the maximum at $X = 0$ for a small λ and two symmetric maxima at about $X = \pm\lambda/2$ as λ is large enough [Fig. 4(a)]; for a fixed λ, $P(X)$ has the maximum at $X = 0$ for a small m and two equal maxima at about $X = \pm\lambda/2$ as m is large enough [Fig. 4(b)]. If the initial state has finite polarization with $r_0^z \neq 0$, we find similar phenomena except that the two maxima of $P(X)$ are unequal and the difference between the two maxima is proportional to r_0^z [Figs. 4(c) and 4(d)].

The probability distribution satisfies the normalization condition

$$Z = \sum_{q=0}^{m} P(q/m - 1/2) = 1. \tag{B10}$$

For a large m, the above integration is overwhelmingly dominated by the maximum term $P_{\max}(q/m - 1/2)$ with $q = mX$, i.e.,
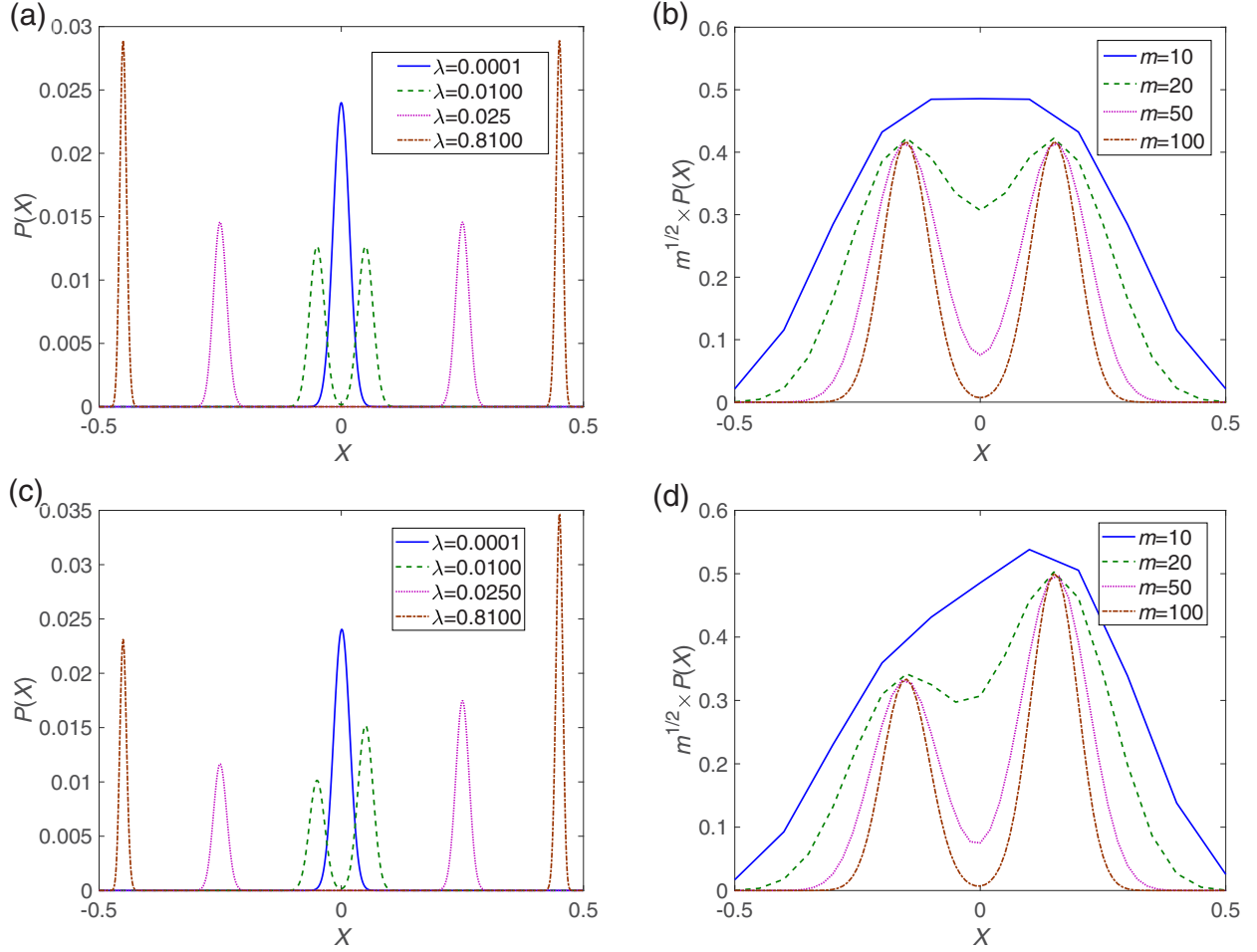
$$Z \approx P_{\max}(X). \tag{B11}$$

FIG. 4. Probability distribution of a sequential POVM. (a) Probability distribution $P(X)$ of measurement polarization X for different measurement strengths λ with the measurement time fixed at $m = 1000$. (b) Modified probability distribution $\sqrt{m}\,P(X)$ of measurement polarization X for different measurement times m with the measurement strength fixed at $\lambda = 0.09$. In (a) and (b), the initial state of the TLS is in the equatorial plane of the Bloch sphere with $r_0^z = 0$ and $r_0 = 1$. (c) and (d) are similar to (a) and (b) but with $r_0^z = 0.2$ and $r_0 = 1$.

We define the free energy as

$$F(X) = -\ln\left[P(X)\right] \approx m\varphi(X) - \ln\left\{\cosh\left[\ln\left(\eta\right)mX\right] + r_0^z \sinh\left[\ln\left(\eta\right)mX\right]\right\}. \tag{B12}$$

To find the maximum term of $P(X)$ is equivalent to finding the minimum term of $F(X)$, which is determined by

$$\frac{\partial F(X)}{\partial X} = m\left\{\ln\left(\frac{1+2X}{1-2X}\right) - \ln\left(\eta\right)\frac{\sinh\left[\ln\left(\eta\right)mX\right] + r_0^z \cosh\left[\ln\left(\eta\right)mX\right]}{\cosh\left[\ln\left(\eta\right)mX\right] + r_0^z \sinh\left[\ln\left(\eta\right)mX\right]}\right\} = 0. \tag{B13}$$

The most interesting phenomenon happens when the initial state of the TLS is in the equatorial plane ($r_0^z = 0$) with the above equation reduced to

$$\frac{\partial F(X)}{\partial X} = m\left\{\ln\left(\frac{1+2X}{1-2X}\right) - \ln\left(\eta\right)\tanh\left[\ln\left(\eta\right)mX\right]\right\} = 0. \tag{B14}$$

Obviously $X = 0$ is a solution of Eq. (B14) and therefore must be a local minimum or maximum point, and if $X = a \neq 0$ is a solution then $X = -a$ is also a solution. The phase transition happens when the solution of Eq. (B14) changes from $X = 0$ to $\pm a$ for a small a, so we can expand Eq. (B14) near $X = 0$:

$$f_1(X) = \ln\left(\frac{1+2X}{1-2X}\right) \approx 4X, \tag{B15}$$

$$f_2(X) = \ln\left(\eta\right)\tanh\left[\ln\left(\eta\right)mX\right] \approx m\ln^2\left(\eta\right)X. \tag{B16}$$
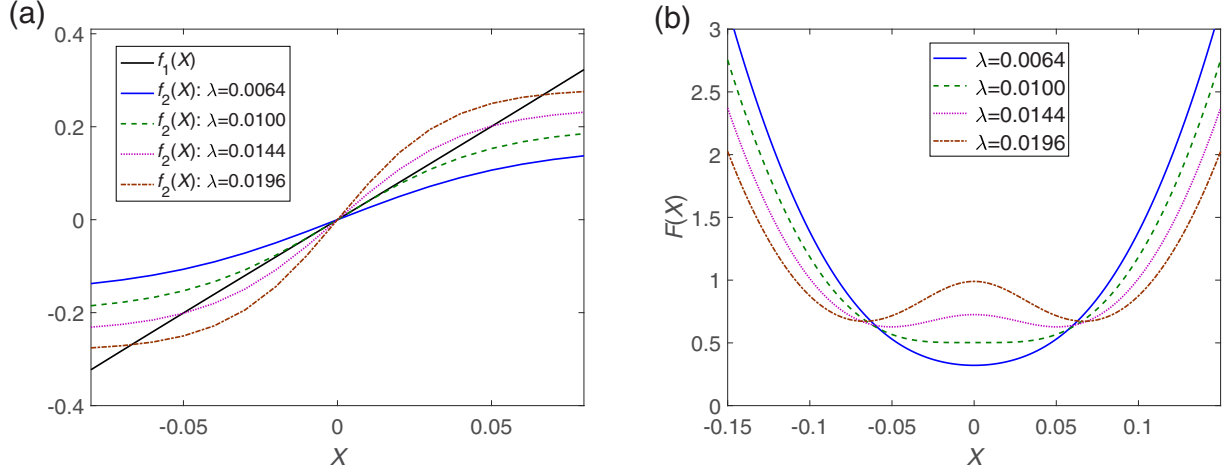
FIG. 5. Determining the minima of free energy of the spin model corresponding to a sequential POVM. (a) The intersections between the two curves $f_1(X) = \ln[(1 + 2X)/(1 - 2X)]$ and $f_2(X) = \ln(\eta) \tanh[\ln(\eta)mX]$, where $\eta = \ln[(1 + \sqrt{\lambda})/(1 - \sqrt{\lambda})]$, determine the free-energy minima. (b) Free energy as a function of the measurement polarization X for different measurement strengths λ. The parameters are such that $m = 1000$, $r_0^z = 0$, and $r_0 = 1$.

As shown in Fig. 5, if $m\ln^2(\eta) < 4$, $f_1(X)$ and $f_2(X)$ have only one intersection and the corresponding free energy has the local minimum at $X = 0$, while, if $m\ln^2(\eta) > 4$, $f_1(X)$ and $f_2(X)$ have two intersections and the free energy has two local minima at $X = \pm a$. So the phase transition happens when $m\ln^2(\eta) = 4$. For weak measurements with small λ, $\ln(\eta) \approx 2\sqrt{\lambda}$, so the phase transition condition is reduced to $m\lambda = 1$.

The measurement polarization X slightly above the critical point can be obtained by expanding $f_1(X)$ and $f_2(X)$ to higher orders:

$$f_1(X) = \ln\left(\frac{1 + 2X}{1 - 2X}\right) \approx 4X + \frac{16}{3}X^3 + \cdots, \tag{B17}$$

$$f_2(X) = \ln(\eta)\tanh[\ln(\eta)mX] \approx m\ln^2(\eta)X - \frac{m^3\ln^4(\eta)}{3}X^3 + \cdots. \tag{B18}$$

By equating $f_1(X)$ and $f_2(X)$ to the third order of X, we obtain the critical measurement polarization:

$$X_c = \pm\sqrt{\frac{3(m\ln^2(\eta) - 4)}{16 + m^3\ln^4(\eta)}}, \quad m\ln^2(\eta) \geqslant 4. \tag{B19}$$

In the weak-measurement regime, the phase boundary becomes $m\lambda = 1$, and the critical measurement polarization becomes $X_c = \pm\sqrt{\frac{3(m\lambda - 1)}{4(1 + m^3\lambda^2)}}$. For a given λ, the critical measurement time is $m_c = 1/\lambda$, and the critical measurement polarization $X_c \propto (m - m_c)^{1/2}$. For a given m, the critical measurement time is $\lambda_c = 1/m$, and the critical measurement polarization $X_c \propto (\lambda - \lambda_c)^{1/2}$. So the critical exponents for the measurement time m and measurement strength λ are both $1/2$.

Moreover, far away from the phase transition point with $m\ln^2(\eta) \gg 4$, $\tanh[\ln(\eta)mX] \approx \pm 1$, so the solution of Eq. (B14) is $X = \pm\sqrt{\lambda}/2$. Near the two stable points $X_{\min} = \pm\sqrt{\lambda}/2$, the free energy can be approximated as

$$F(X) \approx F(X_{\min}) + \frac{\partial F(X_{\min})}{\partial X}(X - X_{\min}) + \frac{1}{2}\frac{\partial^2 F(X_{\min})}{\partial X^2}(X - X_{\min})^2$$

$$= F(\pm\sqrt{\lambda}/2) + \frac{m}{2}\left[\frac{4}{1 - \lambda} - \frac{m\ln^2(\eta)}{\cosh^2[\sqrt{\lambda}\ln(\eta)m/2]}\right](X \mp \sqrt{\lambda}/2)^2, \tag{B20}$$

so the probability distribution can be approximated as a Gaussian distribution:

$$P(X) \approx P(\pm\sqrt{\lambda}/2)\exp\left\{-\frac{m}{2}\left[\frac{4}{1 - \lambda} - \frac{m\ln^2(\eta)}{\cosh^2[\sqrt{\lambda}\ln(\eta)m/2]}\right](X \mp \sqrt{\lambda}/2)^2\right\}. \tag{B21}$$

For a large m, it can be further simplified as

$$P(X) \approx P(\pm\sqrt{\lambda}/2)\exp\left[-\frac{2m}{1 - \lambda}(X \mp \sqrt{\lambda}/2)^2\right] = P(\pm\sqrt{\lambda}/2)\exp\left[-\frac{(X \mp \sqrt{\lambda}/2)^2}{2\sigma^2}\right], \tag{B22}$$

where the standard deviation $\sigma = \sqrt{1-\lambda}/(2\sqrt{m})$ is inversely proportional to the square root of the measurement number m.

3. Effects of initial states of the TLS on the measurement statistics

In the main text, we mainly discuss the measurement statistics when the initial state of the TLS has no polarization, i.e., in the equator of the Bloch sphere with $r_0^z = 0$. In this subsection, we discuss the measurement statistics for the other initial states on the Bloch sphere. If the initial state of the TLS is in the north or south pole with $r_0^z = \pm 1$, then the probability distribution becomes

$$P_{\mathrm{II}}^A(\alpha_1, \alpha_2, \ldots, \alpha_m) = \frac{1}{2^m} \prod_{k=1}^{m} (1 + \sqrt{\lambda}\alpha_0\alpha_k), \tag{B23}$$

with $\alpha_0 = |r_0^z|/r_0^z$. This is just the normalized probability of the configuration $(\alpha_1, \alpha_2, \ldots, \alpha_m)$ for m independent paramagnetic classical spins with the Hamiltonian

$$H_{\mathrm{II}}^A(\alpha_1, \alpha_2, \ldots, \alpha_m) = -\omega\alpha_0 \sum_{k=1}^{m} \alpha_k, \tag{B24}$$

where $\omega = \tanh^{-1}(\sqrt{\lambda})$ is the effective energy of the spins and α_0 determines the magnetic-field direction. So the measurement polarization X can be understood as the average magnetic polarization of all the spins, i.e., $X = \tanh(\omega)/2 = \sqrt{\lambda}/2$, where the free energy of the spin model has the minimum [Fig. 6(a)]. The reason is that the state of the TLS is unchanged by the measurements, as can be seen from Eq. (B7) and Figs. 6(d) and 6(e), so the probability to obtain different results is the same for all the measurements. In this case, there is no phase transition.

If the initial state of the TLS is anywhere on the Bloch sphere other than the north or south poles or the equator with $|r_0^z| \in (0,1)$, in the weak-measurement regime ($\lambda \ll 1$), the probability distribution in Eq. (10) can be mapped to the long-range ferromagnetic Ising model under an external magnetic field up to the leading-order terms ($\propto \lambda$):

$$H_{\mathrm{II}}^B(\alpha_1, \alpha_2, \ldots, \alpha_m) \approx -r_0^z\sqrt{\lambda} \sum_{k=1}^{m} \alpha_k - \lambda \sum_{j<k}^{m} \alpha_j\alpha_k, \tag{B25}$$

where the magnetic field is proportional to the z component of Bloch vector polarization of the initial state. In this case, the free energy becomes unsymmetrical in the polarized phase and therefore the measurement polarization has a preferred value, i.e., $X = \sqrt{\lambda}/2$ ($X = -\sqrt{\lambda}/2$) for $r_0^z > 0$ ($r_0^z < 0$), and the probability in the preferred value is about $(1 + |r_0^z|)/(1 - |r_0^z|)$ times that in the unpreferred value. The measurement polarization X as a function of measurement time m and measurement strength λ changes more and more smoothly as $|r_0^z|$ increases and the phase-transition behaviors gradually disappear [Figs. 6(b) and 6(c)]. Moreover, the final state of the TLS is also gradually polarized toward the north (south) pole for $r_0^z > 0$ ($r_0^z < 0$) as the measurement times or measurement strength increases [Figs. 6(d) and 6(e)].

4. Average measurement polarization and correlation function

For the probability distribution in Eq. (B8), the average polarization for the jth measurement and the correlation function between the jth measurement and the lth measurement ($1 \leqslant j < l \leqslant m$) are

$$\langle \alpha_j \rangle = \sum_{\alpha_1=\pm1} \sum_{\alpha_2=\pm1} \cdots \sum_{\alpha_m=\pm1} \left\{ \frac{\alpha_j}{2^{m+1}} \left[(1 + r_0^z) \prod_{k=1}^{m} (1 + \sqrt{\lambda}\alpha_k) + (1 - r_0^z) \prod_{k=1}^{m} (1 - \sqrt{\lambda}\alpha_k) \right] \right\}$$

$$= \frac{1}{4} \sum_{\alpha_j=\pm1} \left[(1 + r_0^z)(\alpha_j + \sqrt{\lambda}) + (1 - r_0^z)(\alpha_j - \sqrt{\lambda}) \right]$$

$$= r_0^z\sqrt{\lambda}, \tag{B26}$$

$$\langle \alpha_j\alpha_l \rangle = \sum_{\alpha_1=\pm1} \sum_{\alpha_2=\pm1} \cdots \sum_{\alpha_m=\pm1} \left\{ \frac{\alpha_j\alpha_l}{2^{m+1}} \left[(1 + r_0^z) \prod_{k=1}^{m} (1 + \sqrt{\lambda}\alpha_k) + (1 - r_0^z) \prod_{k=1}^{m} (1 - \sqrt{\lambda}\alpha_k) \right] \right\}$$

$$= \frac{1}{8} \sum_{\alpha_j=\pm1} \sum_{\alpha_l=\pm1} \left[(1 + r_0^z)(\alpha_j + \sqrt{\lambda})(\alpha_l + \sqrt{\lambda}) + (1 - r_0^z)(\alpha_j - \sqrt{\lambda})(\alpha_l - \sqrt{\lambda}) \right]$$

$$= \lambda. \tag{B27}$$

So the average polarization for any single measurement is the same and proportional to the initial-state polarization r_0^z and the square root of the measurement strength $\sqrt{\lambda}$, while the correlation function between any two measurements is also the same and equal to the measurement strength λ. These points can be understood as follows.
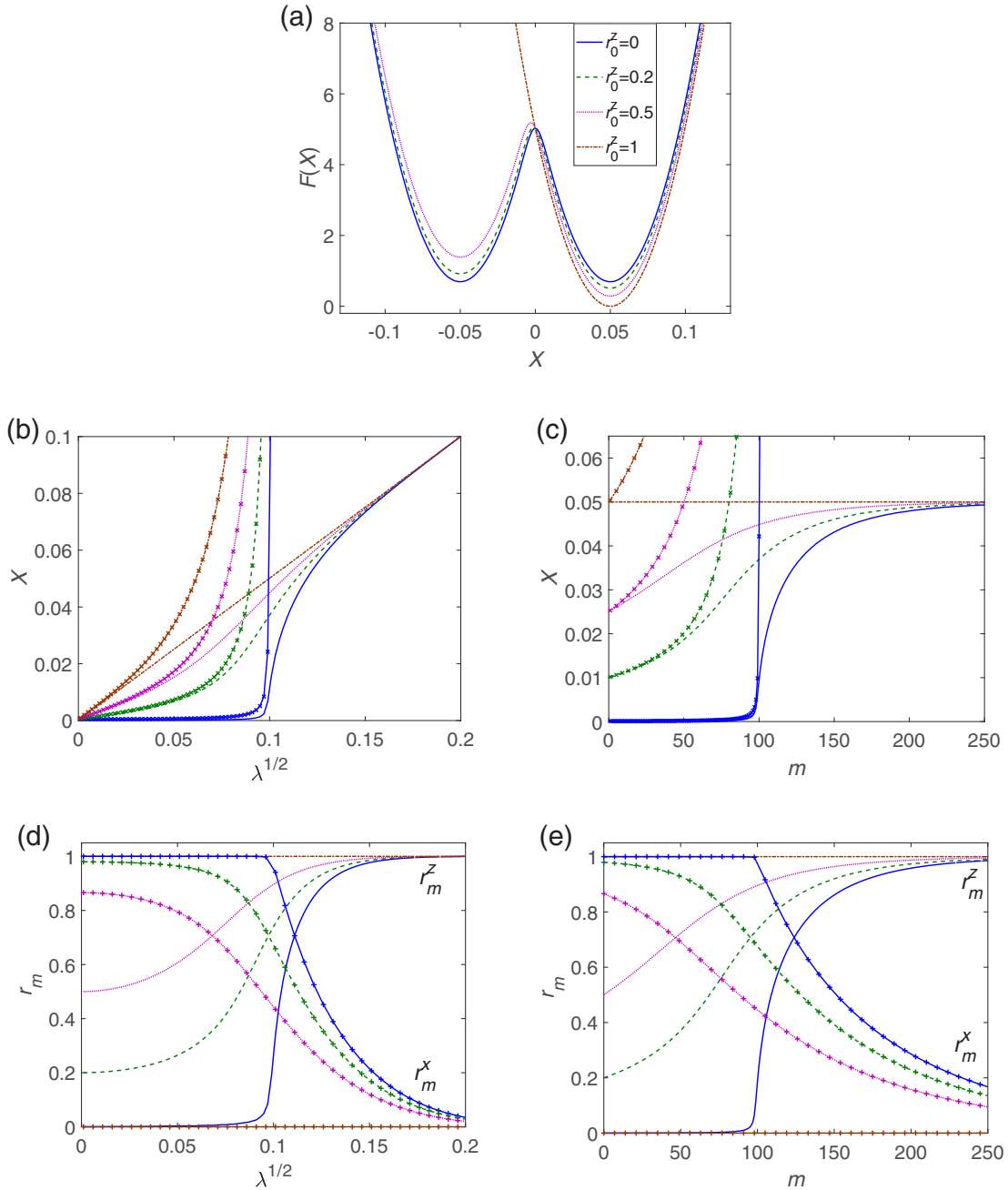
FIG. 6. Effects of initial states on the phase transitions of sequential weak measurement. Different initial states (given by the initial polarization r_0^z) are represented by different line colors. (a) Free energy as a function of the measurement polarization X. The measurement strength and measurement time are $m = 1000$ and $\lambda = 0.01$, respectively. (b), (d) The measurement polarization X and the final Bloch vector polarization r_m as functions of the square root of the measurement strength with measurement times fixed at $m = 100$. (c), (e) The measurement polarization X and the final Bloch vector polarization r_m as functions of the measurement time with the measurement strength fixed at $\lambda = 0.01$. In (b) and (c), the lines without (with) crosses represent the results from the exact model (the approximate long-range Ising model). In (d) and (e), the lines without (with) plus signs represent the z (x) component of the final Bloch vector. Initially the TLS is in a pure state with $r_0 = 1$ and $r_0^y = 0$.

(i) If $r_0^z = 0$, the measurement statistics can be approximated by the long-range ferromagnetic Ising model, where any one spin is equally coupled to all other spins, so the correlation function between any two spins is always the same while the average polarization of any spin is zero since the average over the two symmetry-broken states is also zero.

(ii) If $r_0^z = \pm 1$, the measurement statistics is equivalent to that of independent classical paramagnetic spins with the external field proportional to $\sqrt{\lambda}$, so the average polarization is equal for all spins and proportional to $\sqrt{\lambda}$ while the correlation function is a trivial constant.

(iii) If $|r_0^z| \in (0,1)$, the measurement statistics can be approximated by the long-range ferromagnetic Ising model under an external magnetic field proportional to both r_0^z and $\sqrt{\lambda}$, so the average polarization for each spin is proportional to both r_0^z and $\sqrt{\lambda}$, while any two spins are also equivalent in this model so the correlation function is also a constant.

5. Example: Nuclear spin polarization by an ancillary electron spin

As an example, let us consider an electron spin (e.g., two energy levels of a nitrogen-vacancy electron spin) and a nuclear spin (e.g., a ^{13}C nuclear spin in diamond). The POVM of the nuclear spin in Eq. (7) can be realized by coupling it to the electron spin and then performing projective measurements on the electron spin [24,25]. The Hamiltonian of the electron spin ($S = 1/2$) and the nuclear spin ($I = 1/2$) is

$$H = AS_z I_z + \omega I_z, \tag{B28}$$

where S_z (I_z) is the electron (nuclear) spin operator with eigenstates $|\pm\rangle_e$ ($|\pm\rangle_n$), A is the coupling strength, and ω is the Larmor frequency of the nuclear spin. The target spin evolution operator conditioned on the sensor spin state is $U_n^{(\pm)}(t) = e^{-i(\omega \pm A/2)I_z t}$. We apply the Ramsey sequence [24] to the electron spin with the propagator of the whole system as

$$U(t) = R_e^x(\pi/2)(U_n^{(+)}(t)|+\rangle_{ee}\langle+| + U_n^{(-)}(t)|-\rangle_{ee}\langle-|)R_e^y(\pi/2), \tag{B29}$$

where $R_e^j(\pi/2) = e^{-i\pi S_i/2}(j = x, y)$ denotes the $\pi/2$ pulse for the electron spin along different axes. Suppose the initial state of the whole system is $|+\rangle_e \otimes |\psi_0\rangle$ with $|\psi_0\rangle = C_0^+|+\rangle_n + C_0^-|-\rangle_n$ denoting the initial target spin state, then projective measurement on the sensor spin with $M_e^{(\alpha)} = (I + 2\alpha S_z)/2$ ($\alpha = \pm 1$) is equivalent to a POVM on the nuclear spin, i.e.,

$$M_n^{(\alpha)}|\psi_0\rangle\langle\psi_0|(M_n^{(\alpha)})^\dagger = \text{Tr}_e[M_e^{(\alpha)}U(t)(|+\rangle_{ee}\langle+| \otimes |\psi_0\rangle\langle\psi_0|)U^\dagger(t)(M_e^{(\alpha)})^\dagger], \tag{B30}$$

where $M_n^{(\alpha)} = (U_n^{(+)} - i\alpha U_n^{(-)})/2 = e^{-i(\omega I_z t + \alpha\pi/4)}[\cos(\theta)I + 2\alpha\sin(\theta)I_z]/\sqrt{2}$ with $\theta = At/2$. Note that $M_n^{(\alpha)}$ is the same POVM operator as that in Eq. (8) except that there is an additional evolution operator $e^{-i(\omega I_z t + \alpha\pi/4)}$, which is independent of the measurement results except for a trivial phase factor and has no effect on the probability distribution of the POVM result. By repetitively applying the Ramsey sequence to the electron spin, sequential POVMs are performed on the nuclear spin with the measurement strength tuned by the time delay t between the two $\pi/2$ pulses [24], and the nuclear spin is polarized to $|+\rangle_n$ ($|-\rangle_n$) with the probability equal to the probability amplitude of the initial state $|C_0^+|^2$ ($|C_0^-|^2$). After spontaneous symmetry breaking at $m = m_C$, the nuclear spin will be trapped in the polarized state by the sequential weak measurement.

In realistic experiments, there may be some imperfections: (i) the timing for the sequential Ramsey sequences may not be exactly the same, so that the POVMs may have slightly different measurement strengths, and (ii) the nuclear spin in the TLS may suffer random magnetic fields between successive POVMs, so that sequential POVMs may have slightly different measurement axes. However, as numerically demonstrated in the Supplemental Material [46], the phase transition behaviors are robust against small inhomogeneity of measurement strength and measurement axes.

6. Ferromagnetic phase transitions in the long-range Ising model

The Hamiltonian of the long-range ferromagnetic Ising model can be mapped to the Hamiltonian of a single large spin with $S_z = \sum_{j=1}^m \alpha_j/2$ [38]:

$$H = -\lambda \sum_{j<k}^m \alpha_j \alpha_k = -\lambda \left(2S_z^2 - \frac{m}{2}\right), \tag{B31}$$

where the large spin number S takes value $0, 1, \ldots, m/2$ for even m and $1/2, 3/2, \ldots, m/2$ for odd m, and the spin degeneracy in each large spin subspace is $D(S) = C_m^{m/2-S} - C_m^{m/2-S-1}$ with C_m^j being the binomial coefficient. So the partition function for the long-range Ising model is

$$Z = \text{Tr}\{e^{\lambda(2S_z^2 - m/2)}\} = e^{-m\lambda/2} \sum_{j=0}^m C_m^j e^{2\lambda m^2(j/m-1/2)^2}, \tag{B32}$$

where we have set $\beta = 1/T = 1$. For a large m, the partition function can be written in the integral form as

$$Z \approx e^{-m\lambda/2} m \int_{-1/2}^{1/2} e^{-m\varphi(X)+2m\lambda X^2} dX, \tag{B33}$$

where $\varphi(X) = (1/2 + X)\ln(1/2 + X) + (1/2 - X)\ln(1/2 - X)$. The integration in Z can be solved by the saddle-point approximation. If $m\lambda < 1$, the saddle point appears at $X = 0$ corresponding to the paramagnetic phase, while if $m\lambda > 1$ there are two symmetric saddle points within $(-1/2, 0)$ and $(0, 1/2)$, corresponding to the ferromagnetic phase. So the ferromagnetic phase transition happens when $m\lambda = 1$.

APPENDIX C: ANOTHER KIND OF SEQUENTIAL POVMs

Consider another kind of POVMs with the POVM operators defined as

$$M_{\alpha_k=+1} = |+1\rangle\langle+1|+\cos\varphi_k|-1\rangle\langle-1|,$$
$$M_{\alpha_k=-1} = \sin\varphi_k|-1\rangle\langle-1|, \tag{C1}$$

where $\varphi_k \in [-\pi/2,\pi/2]$. With $|\varphi_k|$ increasing from zero to $\pi/2$, the kth measurement continuously changes from weak measurement to strong projective measurement. This kind of measurement operators can be written in a form similar to that in Eq. (7):

$$M_{\alpha_k} = \frac{1}{\sqrt{2}}[aI + b\sigma_z + \alpha_k(cI + d\sigma_z)] = \frac{1}{\sqrt{2}}[(a + \alpha_k c)I + (b + \alpha_k d)\sigma_z], \tag{C2}$$

with

$$a = (1 + \cos\varphi_k + \sin\varphi_k)/(2\sqrt{2}),$$
$$b = (1 - \cos\varphi_k - \sin\varphi_k)/(2\sqrt{2}),$$
$$c = (1 + \cos\varphi_k - \sin\varphi_k)/(2\sqrt{2}),$$
$$d = (1 - \cos\varphi_k + \sin\varphi_k)/(2\sqrt{2}). \tag{C3}$$

After m sequential measurements, the un-normalized density matrix of the TLS is

$$\rho_k = \mathcal{M}_{\alpha_k} \cdots \mathcal{M}_{\alpha_2}\mathcal{M}_{\alpha_1}\rho_0 = A_k + B_k\hat{\boldsymbol{\sigma}} \cdot \boldsymbol{n}_k, \tag{C4}$$

and the normalized density matrix is $\rho_k' = \rho_k/\text{Tr}(\rho_k) = (I + r_k\hat{\boldsymbol{\sigma}} \cdot \boldsymbol{n}_k)/2$ with $r_k = B_k/A_k$ and $\boldsymbol{n}_k$ denoting the length and direction of the Bloch vector, respectively. The relation between ρ_k and ρ_{k-1} is fully captured by the transfer matrix

$$\begin{bmatrix} A_k \\ B_k^x \\ B_k^y \\ B_k^z \end{bmatrix} = \frac{1}{2}\begin{bmatrix} 1 + \alpha_k\cos^2\varphi_k & 0 & 0 & \alpha_k\sin^2\varphi_k \\ 0 & (1 + \alpha_k)\cos\varphi_k & 0 & 0 \\ 0 & 0 & (1 + \alpha_k)\cos\varphi_k & 0 \\ \alpha_k\sin^2\varphi_k & 0 & 0 & 1 + \alpha_k\cos^2\varphi_k \end{bmatrix}\begin{bmatrix} A_{k-1} \\ B_{k-1}^x \\ B_{k-1}^y \\ B_{k-1}^z \end{bmatrix}. \tag{C5}$$

So the solution can be obtained in a way similar to that in Appendix B 1:

$$A_m = \frac{1}{2^{m+2}}\left\{\left(1 + r_0^z\right)\prod_{k=1}^{m}(1 + \alpha_k) + \left(1 - r_0^z\right)\prod_{k=1}^{m}[1 + \alpha_k\cos(2\varphi_k)]\right\},$$

$$B_m^x = \frac{1}{2^{m+1}}r_0^x\prod_{k=1}^{m}[(1 + \alpha_k)\cos\varphi_k],$$

$$B_m^y = \frac{1}{2^{m+1}}r_0^y\prod_{k=1}^{m}[(1 + \alpha_k)\cos\varphi_k],$$

$$B_m^z = \frac{1}{2^{m+2}}\left\{\left(1 + r_0^z\right)\prod_{k=1}^{m}(1 + \alpha_k) + \left(1 - r_0^z\right)\prod_{k=1}^{m}[1 + \alpha_k\cos(2\varphi_k)]\right\}. \tag{C6}$$

The probability distribution is

$$P_{\text{III}}(\alpha_1,\alpha_2,\ldots,\alpha_m) = \text{Tr}[\rho_m] = 2A_m$$
$$= \frac{1}{2^{m+1}}\left[\left(1 + r_0^z\right)\prod_{k=1}^{m}(1 + \alpha_k) + \left(1 - r_0^z\right)\prod_{k=1}^{m}[1 + \alpha_k\cos(2\varphi_k)]\right]. \tag{C7}$$

The density matrix of the TLS after m measurements is $\rho_m' = (I + r_m\hat{\boldsymbol{\sigma}} \cdot \boldsymbol{n}_m)/2$ with

$$r_m^x = \frac{B_m^x}{A_m} = \frac{2r_0^x\prod_{k=1}^{m}[(1 + \alpha_k)\cos\varphi_k]}{\left(1 + r_0^z\right)\prod_{k=1}^{m}(1 + \alpha_k) + \left(1 - r_0^z\right)\prod_{k=1}^{m}[1 + \alpha_k\cos(2\varphi_k)]},$$

$$r_m^y = \frac{B_m^y}{A_m} = \frac{2r_0^y\prod_{k=1}^{m}[(1 + \alpha_k)\cos\varphi_k]}{\left(1 + r_0^z\right)\prod_{k=1}^{m}(1 + \alpha_k) + \left(1 - r_0^z\right)\prod_{k=1}^{m}[1 + \alpha_k\cos(2\varphi_k)]}, \tag{C8}$$

$$r_m^y = \frac{B_m^z}{A_m} = \frac{\left(1 + r_0^z\right)\prod_{k=1}^{m}(1 + \alpha_k) - \left(1 - r_0^z\right)\prod_{k=1}^{m}[1 + \alpha_k\cos(2\varphi_k)]}{\left(1 + r_0^z\right)\prod_{k=1}^{m}(1 + \alpha_k) + \left(1 - r_0^z\right)\prod_{k=1}^{m}[1 + \alpha_k\cos(2\varphi_k)]}.$$

APPENDIX D: SEQUENTIAL MULTIOUTCOME POVMs

The previous cases are all about sequential binary-outcome POVMs. However, the POVMs even on a TLS can have multiple outcomes, so a natural problem is to investigate the measurement statistics of such sequential multioutcome POVMs, and their possible connection with the Boltzmann distribution of Ising models of higher spins. In this case, we consider m successive commuting $(2S + 1)$-outcome POVMs with the kth POVM operator defined as

$$M_{\alpha_k} = x_k I + y_k \alpha_k \sigma_z, \tag{D1}$$

where x_k and y_k are real positive parameters, $\alpha_k = -2S, -2S + 1, \ldots, 2S$ for S being a half integer, and $\alpha_k = -S, -S + 1, \ldots, S$ for S being an integer. The normalization condition $\sum_{\alpha_k} M_{\alpha_k}^\dagger M_{\alpha_k} = I$ requires that $x_k^2(2S + 1) + y_k^2 \sum_{\{\alpha_k\}} \alpha_k^2 = 1$.

Suppose the initial state of the TLS is $|\psi_0\rangle = C_0^+|+1\rangle + C_0^-|-1\rangle$ with $|\pm1\rangle$ being the eigenstate of σ_z and $|C_0^+|^2 + |C_0^-|^2 = 1$. The un-normalized state of the TLS after m measurements is

$$|\psi_m\rangle = M_{\alpha_m} \cdots M_{\alpha_2} M_{\alpha_1} |\psi_0\rangle = C_m^+|+1\rangle + C_m^-|-1\rangle, \tag{D2}$$

with

$$C_m^\pm = (x_m \pm y_m \alpha_m) C_{m-1}^\pm = C_0^\pm \prod_{k=1}^m (x_k \pm y_k \alpha_k), \tag{D3}$$

and the normalized state is $|\psi'_m\rangle = |\psi_m\rangle / \sqrt{\langle \psi_m | \psi_m \rangle}$. With the Bloch vector components of the final state defined as $r_m^i = \langle \sigma_i \rangle = \langle \psi'_m | \sigma_i | \psi'_m \rangle$ $(i = x, y, z)$ $(r_m = 1$ for a pure state), the probability distribution for the measurement results is analytically derived as

$$P_{\text{IV}} = \frac{1 + r_0^z}{2} \prod_{k=1}^m \left(x_k^2 + y_k^2 \alpha_k^2 + 2x_k y_k \alpha_k \right) + \frac{1 - r_0^z}{2} \prod_{k=1}^m \left(x_k^2 + y_k^2 \alpha_k^2 - 2x_k y_k \alpha_k \right), \tag{D4}$$

where $r_0^z = |C_0^+|^2 - |C_0^-|^2$ is the z component of the Bloch vector of the initial state. Assume that all the sequential POVMs are the same with $x_1 = x_2 = \cdots = x_m = x$ and $y_1 = y_2 = \cdots = y_m = y$, and all weak measurements with $y \ll x \approx (2S + 1)^{-1/2}$. With the notation $\mu = y/x \leqslant 1$, the probability distribution is written as

$$P_{\text{IV}} = \frac{x^{2m}}{2} \left[(1 + r_0^z) \prod_{k=1}^m \left(1 + \mu^2 \alpha_k^2 + 2\mu \alpha_k \right) + (1 - r_0^z) \prod_{k=1}^m \left(1 + \mu^2 \alpha_k^2 - 2\mu \alpha_k \right) \right], \tag{D5}$$

The lattice spin Hamiltonian corresponding to the probability distribution of the sequential POVMs is

$$H_{\text{IV}} = -\ln \left\{ \frac{x^{2m}}{2} \left[(1 + r_0^z) \prod_{k=1}^m \left(1 + \mu^2 \alpha_k^2 + 2\mu \alpha_k \right) + (1 - r_0^z) \prod_{k=1}^m \left(1 + \mu^2 \alpha_k^2 - 2\mu \alpha_k \right) \right] \right\}. \tag{D6}$$

To the second order of μ, the Hamiltonian can be approximated as

$$H_{\text{IV}} \approx -\sum_{k=1}^m \left(r_0^z \mu \alpha_k + \mu^2 \alpha_k^2 \right) - 4\mu^2 \sum_{j<k} \alpha_j \alpha_k, \tag{D7}$$

where we have neglected the trivial constant $-2m \ln x$ in H_{IV}. Such a Hamiltonian describes the long-range spin-S Ising model [47–49], which is known to have phase transitions similar to those of long-range spin-1/2 Ising models. Thus phase transitions from weak to strong measurement are expected in sequential multioutcome POVMs.

---

[1] M. Schlosshauer, Decoherence, the measurement problem, and interpretations of quantum mechanics, Rev. Mod. Phys. **76**, 1267 (2005).

[2] W. H. Zurek, Decoherence, einselection, and the quantum origins of the classical, Rev. Mod. Phys. **75**, 715 (2003).

[3] M. D. Srinivas, *Measurements and Quantum Probabilities* (Universities Press, Hyderabad, India, 2001).

[4] M. R. Pahlavani, *Measurements in Quantum Mechanics* (InTech, Rijeka, Croatia, 2012).

[5] J. Cotler, C.-M. Jian, X.-L. Qi, and F. Wilczek, Superdensity operators for spacetime quantum mechanics (unpublished).

[6] M. A. Nielsen and I. L. Chuang, *Quantum Computation and Quantum Information* (Cambridge University Press, Cambridge, England, 2000).

[7] N. Gisin, G. Ribordy, W. Tittel, and H. Zbinden, Quantum cryptography, Rev. Mod. Phys. **74**, 145 (2002).

[8] C. L. Degen, F. Reinhard, and P. Cappellaro, Quantum sensing, Rev. Mod. Phys. **89**, 035002 (2017).

[9] J. M. Elzerman, R. Hanson, L. H. W. van Beveren, B. Witkamp, L. M. K. Vandersypen, and L. P. Kouwenhoven, Single-shot read-out of an individual electron spin in a quantum dot, Nature (London) **430**, 431 (2004).

[10] A. N. Vamivakas, C.-Y. Lu, C. Matthiesen, Y. Zhao, S. Fält, A. Badolato, and M. Atatüre, Observation of spin-dependent quantum jumps via quantum dot resonance fluorescence, Nature (London) **467**, 297 (2010).

[11] P. Neumann, J. Beck, M. Steiner, F. Rempp, H. Fedder, P. R. Hemmer, J. Wrachtrup, and F. Jelezko, Single-shot readout of a single nuclear spin, Science **329**, 542 (2010).

[12] A. Morello, J. J. Pla, F. A. Zwanenburg, K. W. Chan, K. Y. Tan, H. Huebl, M. Möttönen, C. D. Nugroho, C. Yang, J. A. van Donkelaar, A. D. C. Alves, D. N. Jamieson, C. C. Escott, L. C. L. Hollenberg, R. G. Clark, and A. S. Dzurak, Single-shot readout of an electron spin in silicon, Nature (London) **467**, 687 (2010).

[13] L. Jiang, J. S. Hodges, J. R. Maze, P. Maurer, J. M. Taylor, D. G. Cory, P. R. Hemmer, R. L. Walsworth, A. Yacoby, A. S. Zibrov, and M. D. Lukin, Repetitive readout of a single electronic spin via quantum logic with nuclear spin ancillae, Science **326**, 267 (2009).

[14] H. M. Wiseman and G. J. Milburn, *Quantum Measurement and Control* (Cambridge University Press, Cambridge, England, 2010).

[15] K. Jacobs and D. A. Steck, A straightforward introduction to continuous quantum measurement, Contemp. Phys. **47**, 279 (2006).

[16] M. B. Mensky, Quantum restrictions for continuous observation of an oscillator, Phys. Rev. D **20**, 384 (1979).

[17] P. Goetsch and R. Graham, Linear stochastic wave equations for continuously measured quantum systems, Phys. Rev. A **50**, 5242 (1994).

[18] S. A. Gurvitz, Measurements with a noninvasive detector and dephasing mechanism, Phys. Rev. B **56**, 15215 (1997).

[19] A. N. Korotkov, Continuous quantum measurement of a double dot, Phys. Rev. B **60**, 5737 (1999).

[20] S. Ashhab, J. Q. You, and F. Nori, The information about the state of a qubit gained by a weakly coupled detector, New J. Phys. **11**, 083017 (2009).

[21] R.-B. Liu, S.-H. Fung, H.-K. Fung, A. N. Korotkov, and L. J. Sham, Dynamics revealed by correlations of time-distributed weak measurements of a single spin, New J. Phys. **12**, 013018 (2010).

[22] A. N. Korotkov, Selective quantum evolution of a qubit state due to continuous measurement, Phys. Rev. B **63**, 115403 (2001).

[23] M. S. Blok, C. Bonato, M. L. Markham, D. J. Twitchen, V. V. Dobrovitski, and R. Hanson, Manipulating a qubit through the backaction of sequential partial measurements and real-time feedback, Nat. Phys. **10**, 189 (2014).

[24] P. C. Maurer, G. Kucsko, C. Latta, L. Jiang, N. Y. Yao, S. D. Bennett, F. Pastawski, D. Hunger, N. Chisholm, M. Markham, D. J. Twitchen, J. I. Cirac, and M. D. Lukin, Room-temperature quantum bit memory exceeding one second, Science **336**, 1283 (2012).

[25] G.-Q. Liu, J. Xing, W.-L. Ma, P. Wang, C.-H. Li, H. C. Po, R.-B. Liu, and X.-Y. Pan, Single-Shot Readout of a Nuclear Spin Weakly Coupled to a Nitrogen-Vacancy Center, Phys. Rev. Lett. **118**, 150504 (2017).

[26] O. Oreshkov and T. A. Brun, Weak Measurements are Universal, Phys. Rev. Lett. **95**, 110409 (2005).

[27] A. N. Jordan and A. N. Korotkov, Qubit feedback and control with kicked quantum nondemolition measurements:

A quantum Bayesian analysis, Phys. Rev. B **74**, 085307 (2006).

[28] A. Chantasri, J. Dressel, and A. N. Jordan, Action principle for continuous quantum measurement, Phys. Rev. A **88**, 042110 (2013).

[29] A. Chantasri and A. N. Jordan, Stochastic path-integral formalism for continuous quantum measurement, Phys. Rev. A **92**, 032125 (2015).

[30] C. Presilla, R. Onofrio, and U. Tambini, Measurement quantum mechanics and experiments on quantum Zeno effect, Ann. Phys. **248**, 95 (1996).

[31] K. Huang, *Statistical Mechanics* (Wiley, New York, 1987).

[32] P. Facchi, S. Pascazio, and F. V. Pepe, Quantum typicality and initial conditions, Phys. Scr. **90**, 074057 (2015).

[33] S. Goldstein, J. L. Lebowitz, R. Tumulka, and N. Zanghì, Canonical Typicality, Phys. Rev. Lett. **96**, 050403 (2006).

[34] C. Bartsch and J. Gemmer, Dynamical Typicality of Quantum Expectation Values, Phys. Rev. Lett. **102**, 110403 (2009).

[35] E. Schrödinger, An undulatory theory of the mechanics of atoms and molecules, Phys. Rev. **28**, 1049 (1926).

[36] E. Schrödinger, *Statistical Thermodynamics* (Cambridge University Press, Cambridge, England, 1952).

[37] R. J. Baxter, *Exactly Solved Models in Statistical Mechanics* (Academic Press, New York, 1982).

[38] B.-B. Wei, C. Burk, J. Wrachtrup, and R.-B. Liu, Magnetic ordering of nitrogen-vacancy centers in diamond via resonator-mediated coupling, EPJ Quantum Technol. **2**, 18 (2015).

[39] H. F. Hofmann, Sequential measurements of non-commuting observables with quantum controlled interactions, New J. Phys. **16**, 063056 (2014).

[40] S. Lloyd, V. Giovannetti, and L. MacCone, Sequential Projective Measurements for Channel Decoding, Phys. Rev. Lett. **106**, 250501 (2011).

[41] S. Dhar and S. Dasgupta, Measurement-induced phase transition in a quantum spin system, Phys. Rev. A **93**, 050103(R) (2016).

[42] J. Dressel, A. Chantasri, A. N. Jordan, and A. N. Korotkov, Arrow of Time for Continuous Quantum Measurement, Phys. Rev. Lett. **119**, 220507 (2017).

[43] M. Morikawa and A. Nakamichi, Quantum measurement driven by spontaneous symmetry breaking, Prog. Theor. Phys. **116**, 679 (2006).

[44] M. Grady, Spontaneous symmetry breaking as the mechanism of quantum measurement, arXiv:hep-th/9409049.

[45] Here we have used Sterling's formula $\ln m! \approx m(\ln m - 1)$ for large m and dropped the trivial term $-m\ln[(1-\lambda)/4]$ independent of X.

[46] See Supplemental Material at http://link.aps.org/supplemental/10.1103/PhysRevA.98.012117 for some Monte Carlo trajectories of sequential POVMs, effects of measurement strength inhomogeneity, and measurement axis inhomogeneity on the phase transitions of sequential POVMs.

[47] F. Y. Wu, The Potts model, Rev. Mod. Phys. **54**, 235 (1982).

[48] R. J. Baxer, *Exactly Solved Models in Statistical Mechanics* (Academic Press, San Diego, 1982).

[49] J. Strecka and M. Jascur, A brief account of the Ising and Ising-like models: Mean-field, effective-field and exact results, Acta Phys. Slovaca **65**, 235 (2015).